SUPERRESOLUTION USING AN ACTIVE ANTENNA ARRAY

U. Nickel

Forschungsinstitut für Funk und Mathematik (FFM) of FGAN, F.R. Germany

INTRODUCTION

The limited resolution of radar antennas is the reason for several errors. Besides tracking errors for formations of targets or jammers, we have multipath and glint errors, which are caused by insufficient resolution. An active antenna array offers the potential for angular superresolution if the sequence of spatial samples of the received waves is available. From spectral analysis and other fields superresolution methods like the maximum-entropy method, Capon's maximum-likelihood method, or spectra generated by eigenvectors are well known. These methods can also be applied for angular resolution with some modifications. Essentially these methods generate a peaky estimate of the angular spectrum. The resolution task then is still left to the user who has to interpret the spectrum. A decision rule for the detection and resolution of peaks with these superresolution methods is to date not known. In addition these methods are only applicable for stationary stochastic signals. The important case of superposed pure sinusoids is not in this class. For automatic signal processing fixed algorithms with well defined properties are necessary. Such algorithms can be found by parameterising the signal with the desired parameters and by fitting this signal model directly to the measured data. The more we specialise the signal model, the better the achievable resolution will be. But the resolution may perhaps be much worse, if the data do not belong to the chosen model. This dilemma is common to all superresolution methods. The signal model should just comprise the essential features to give a powerful superresolution method. For radar with narrow-band receivers a point-target model seems appropriate. This model leads to angular spectral line fitting to the data.

RESOLUTION AS A DECISION PROBLEM

Model fitting is a decision problem. The formulation of radar resolution as a decision problem has been attacked by several authors e.g. Root (1), Ksienski and McGhee (2), Birgenheier (3), and others. The output of an antenna array is a time sequence of vectors. It is essential to formulate the decision problem for a given set not only of spatial but also temporal samples. The narrow-band point target signal model is still open for several fluctuations of the signal amplitude and phase. No assumptions should be made on these fluctuations because they may differ from one application to another. Therefore we consider the amplitudes and phases as a deterministic, but unknown sequence. Assuming measured data of the form signal plus pure receiver noise, we can formulate hypotheses (i.e. families of distributions of the data) and we have to decide from which class the data were taken from.

Multi-hypothesis test. It can be shown that a solution of this multi-hypothesis problem can be given by a sequence of likelihood-ratio tests of the following form: We test the hypothesis "the number of targets is $\leq$ M" against the alternative "the number of targets is > M" starting with M=0 and increasing the number of targets M. Once we have accepted the hypothesis "the number of targets is $\leq$ M", we stop testing. The decision for the target number is M. In this way the multi-hypothesis test is sequential with respect to the number M. The overall procedure is shown in figure 1. A precise formulation of the hypotheses, the test problem, and the solution can be given and will be published elsewhere. The likelihood ratio test has the advantage of giving a fixed asymptotic error level, in contrast to the general Bayes approach. For further data processing, like tracking algorithms, this is important. If the test procedure is terminated at some stage M, before the decision has been made, one has at least the information that the number of targets is greater than M. This information may sometimes be useful. To compute the likelihood ratio, at each stage M a maximum likelihood parameter estimation has to be carried out, which essentially estimates the directions of the targets for the assumed number M. There are several applications where a test procedure is not needed, e.g. for multipath error reduction a two target model may be sufficient. The procedure is then simpler.

ESTIMATION OF THE DIRECTION

Signal model. Suppose we have given M point sources in the farfield of the antenna. For an array with elements at the positions x_i, y_i, i=1,...N, the complex sample ouput at the i-th element then can be written

$$z_i = \sum_{k=1}^{M} \beta_k e^{j\phi_k} e^{-j2\pi/\lambda(x_i u_k + y_i v_k)} + n_i$$

where u_k, v_k denote the direction cosines for azimut and elevation. λ is the wavelength and n the receiver noise sample ($j^2=-1$). In vector notation we can write this equation as

$\underline{z} = \underline{A}\ \underline{b} + \underline{n}$, where $b_k = \beta_k e^{j\phi_k}$, and the

transmission matrix $\underline{A}$ has the elements

$$e^{-j2\pi/\lambda(x_i u_k + y_i v_k)} \qquad (i=1,..N,\ k=1,..M)$$

(vectors and matrices are underlined). Signal models other than $\underline{A}\underline{b}$ are also possible, the matrix $\underline{A}$ can have another form.

Maximum likelihood estimation

For white gaussian uncorrelated receiver noise maximum likelihood estimation leads to the minimisation of the mean squared error between the measured data and the signal model. For K data vectors $\underline{z}$ we have to minimise

$$\sum_{k=1}^{K} \| \underline{z}_k - \underline{A}\ \underline{b} \|^2 \qquad (1)$$

(‖..‖ denotes the square norm for complex vectors.) The minimisation with respect to $\underline{b}$ has to be done for each $\underline{z}_k$, because the amplitudes and phases are assumed to be an unknown, deterministic sequence. This is a linear least squares problem and the solution can be written down at once: $\hat{\underline{b}}_k = (\underline{A}^* \underline{A})^{-1} \underline{A}^* \underline{z}_k$. (..* denotes complex- conjugate transpose). We are thus left with the minimisation of the function

$$Q(\underline{u},\underline{v}) = \sum_{k=1}^{K} \| \underline{z}_k - \underline{A} (\underline{A}^* \underline{A})^{-1} \underline{A}^* \underline{z}_k \|^2 \quad (2)$$

Equivalently we could maximise

$$S(\underline{u},\underline{v}) = \sum_{k=1}^{K} \underline{z}_k^* \underline{A} (\underline{A}^* \underline{A})^{-1} \underline{A}^* \underline{z}_k \quad (3)$$

Function (3) shows that this estimation is a generalisation of conventional beamforming which is the case M=1. We have to maximise the square of a vector of M simultaneous decoupled sum-beams. For the derivation of these functions we have assumed omnidirectional patterns of the antenna elements. If the single elements have a directional, but equal pattern, we would have to replace the matrix $\underline{A}$ by a matrix $\underline{A}\,\underline{C}$, with $\underline{C}$ a diagonal (MxM)-matrix, depending on the directions. The form of the functions (3), (4) shows that these functions are invariant under such left-side transformations $\underline{C}$ of the matrix $\underline{A}$ (as long as $\underline{C}$ is regular). Equal antenna element patterns therefore always lead to the same minimisation problem. As a consequence mutual coupling effects do not influence the estimation procedure, if the coupling effects are the same for all elements (e.g. for large arrays on a regular grid). One single snapshot $\underline{z}$ is in principle sufficient for this kind of resolution, if the signal-to-noise ratio is high enough. No assumptions have been made on the $\underline{b}_k$, they may be deterministic or stochastic. Direction finding by maximising (minimising) these functions may be considered as the optimum procedure, but it is very time consuming and for most radar applications of less value. The main problem of this kind of resolution is the maximisation (minimisation) of the function (2) or (3).

Suboptimum estimation

From equation(2),(3) we can derive a simple, suboptimum estimation algorithm. We can minimise Q for only one observation (K=1) with a gradient algorithm, but we use a new observation $\underline{z}$ for each iteration step. Thus the iteration proceeds in the direction of steepest descent, but the underlying function is time varying. This leads to a stochastic approximation algorithm

$$\underline{w}_{k+1} = \underline{w}_k - a_k \underline{G}(\underline{z}_k, \underline{w}_k) \;;\; k=1,2,3... \quad (4)$$

where $\underline{w}_k = (\underline{u}_k, \underline{v}_k)$ and

$\underline{G}(\underline{w}_k, \underline{z}_k) = \text{grad}\, \underline{Q}(\underline{w}_k, \underline{z}_k)$

and a_k is a sequence of real numbers with

$\Sigma\, a_k = \infty$, $\Sigma\, a_k^2 < \infty$ to achieve

convergence with probability 1. A sequence a_k = const/k has the desired properties. The double null tracker of White (4) is a special case of this algorithm. Conditions for convergence with probability 1 can be found in the literature. The convergence point is that set of directions $\tilde{\underline{w}}$ with $E\{\underline{G}(\tilde{\underline{w}},\underline{z})\} = \underline{0}$. If $\underline{G}$ = grad $\underline{Q}$, convergence properties can therefore be studied by dicussing the function E{Q} for various fluctuations of the signal amplitude and phase. To ensure convergence, the iteration has to be bounded to a convergence region, which can be chosen to be the disk of the antenna beamwidth. This region is found by scanning the conventional sum-beam (the stage M=1 in the procedure of fig.1). The iteration (4) has the advantage that only one observation vector $\underline{z}$ has to be stored (in contrast to equ.(2) or (3)). In effect the gradient depends only on M simultaneous sum- and difference-beams in the directions $\underline{w}$. Figure 2 shows the computations for the gradient $\underline{G}$ for the case M=2 and a linear antenna. Without beamforming (which should be done by special analog or digital hardware) 8 complex multiplications and 4 additions are necessary for one iteration step for this example. For M=1 the algorithm simply tries to null the difference beam.

Experimental results

Computer Simulations. For the simulations shown here we used an antenna consisting of 192 elements and a diameter of 37λ. The location of the elements with a slight parabolic density tapering is shown in figure 3. Figure 4 shows the estimation of the azimut direction cosines u with a version of the stochastic approximation algorithm for two given targets. The elevation estimation looks quite similar. The 2 targets are located at $\tilde{\underline{u}}$ = (-0.35 BW/2, 0.35 BW/2), $\tilde{\underline{v}}$ = (-0.35 BW/2, 0.35 BW/2).The starting point of the iteration is always $\underline{u}$ =(0,0), $\underline{v}$ = (-0.9 BW/2, 0.9 BW/2). Figure 4(a) shows the estimation for uncorrelated targets with Rayleigh-fluctuating amplitudes, figure 4(b) with fixed amplitudes and a constant phase difference of 0 degree. The antenna output signal-to-noise ratio is 19.8dB. Large numbers of element outputs are often pre-processed by forming subgroups. We may consider these subgroups as new antenna elements with certain antenna patterns. The estimation procedure can then be applied for this element configuration. If the subgroups are chosen to be all equal, these new elements have equal patterns. The estimation therefore remains the same as mentioned above. We have only to use the center of gravity of the subgroups as element positions. Unequal subgroups affect the estimation. The transmission matrix $\underline{A}$ then needs a correction. Figure 4(c) shows the estimation using only subgroup outputs without any correction. The 192-element antenna was divided into 24 subgroups, each consisting of 8 elements as indicated in figure 3. This result shows that empirically the estimation by stochastic approximation is robust against small errors of the transmission matrix $\underline{A}$.

Measured 2 target signals. Further tests were made with an experimental setup. To measure 2-target configurations, a 6-element antenna at S-band with 2λ diameter was taken. 5 elements were located at the corners of a pentagon and one element at the center. The 12 element outputs (I and Q channels) were converted analog to digital with 8 bits and then processed by a desk computer. Targets were simulated by two transmit elements of 1m separation. These were located in front of the antenna at a distance of ca. 4m. Figure 5 shows the configuration. The 2 targets were simulated by 2 doppler-shifted pure sinusoids. Figure 6 shows the estimation. The above part shows the conventional azimut sum-beam patterns if only one of the 2 transmit elements is active (gross lines) and 3 patterns by superposition of the two sources for some random phase differences. Below is shown the azimut and elevation estimation of the directions by stochastic approximation with 30 iterations. The circle indicates the size of the 3 dB beamwidth. The estimated directions differ from the maxima of the single-target sum-beam patterns by 0.02 of the 3dB-beamwidth. The signal-to-noise ratio in this case was very high. The main errors were due to misadjustment, channel quantisation, and multipath effects.

TEST FOR THE NUMBER OF TARGETS

With the directions estimated by the sub-optimum stochastic approximation, we are no longer able to perform a likelihood-ratio test, which would give a fixed asymptotic error level. Nevertheless we can find a test statistic which uses the suboptimum estimation of the directions, for testing the hypotheses under consideration H : " $M < \hat{M}$ " against K :" $M > \hat{M}$". This statistic is the value of (2) $Q(\hat{\underline{u}}, \hat{\underline{v}})$, where $(\hat{\underline{u}}, \hat{\underline{v}})$ are found by stochastic approximation. In this case K can be small, e.g. K=2,3,4. $Q(\hat{\underline{u}}, \hat{\underline{v}})$ measures the residual energy after signal extraction.

Test at approximate error level. If the estimation is sufficiently accurate, we can approximate the distribution of Q by a χ^2-distribution with 2K(N-M) degrees of freedom, because then Q is only a sum of squares of 2K(N-M) noise samples. This is because

$$(\underline{I} - \underline{A}(\underline{A}^* \underline{A})^{-1} \underline{A}^*) \underline{s} = \underline{0} \qquad (\underline{s} = \underline{A}\underline{b})$$

We are thus able to construct a sequence of tests at an approximate level of probability of error of the first kind for each stage $\hat{M}$ (i.e. $P\{Q > \eta_{\hat{M};\alpha}\} < \alpha$ if H_M is given). The sequential form of the multi-hypothesis test of fig.1 then yields that for the overall type-1-error probability for a given target number M, we have also $P\{\hat{M} > M\} < \alpha$, because if H_M is valid, we have :

$$P\{\hat{M} > M\} = P\{Q > \eta_{1;\alpha}\} P\{Q > \eta_{2;\alpha}\} \cdot\cdot P\{Q > \eta_{M;\alpha}\} < \alpha . \qquad (5)$$

We have thus constructed a multi-hypothesis test which has approximately a given level of error $P\{\hat{M} > M\}$. For target resolution the computation of the set of thresholds $\eta_{M;\alpha}$ is essential, because these thresholds cannot be adjusted experimentally when the radar is in operation, as is often done for single target detection. Multiple target situations are in general too rare. In the case of Rayleigh-fluctuating targets with uniformly distributed phase differences we can even compute an approximation of the probability of detecting the correct number, because under H_M, $P\{Q > \eta_{L;\alpha}\}$ for L<M can be computed. If we set $P\{Q < \eta_{M;\alpha}\} = 1 - \alpha$ in equation (5), we get a lower bound of this overall probability of detection. Computer simulations showed that for 2 targets the computed probability of detection gave a reasonable good approximation for the observed probability of detection. For targets with fixed amplitudes the simulations gave a higher probability of detection, so that the computed probability in this case may also be considered as a lower bound. Figure 7 shows this computed probability of detection as a function of the output signal-to noise ratio (SNR) for the 192-element antenna and 2 given targets. The different curves are for different target separations, varying from 1.2 to 0.4 degrees in steps of 0.2 degrees. The 3dB beamwidth of the 192-element antenna is approximately 1.6 degrees. Averaging of the residual error was done with only 2 samples (the function Q of equ. (2) taken with K=2). The level α is 0.04 and 0.08. One can see that in this case a SNR of 20 dB gives a sufficiently high probability of detection. By the $1/R^4$-law we can reach such values for the SNR at 0.4 times the distance with a SNR of 3dB. Further averaging increases the probability of detection.

CONCLUSIONS

We have shown that using an active antenna array a resolution enhancement over the conventional 3-dB beamwidth by signal processing is in principle possible under the assumption of a point target model. The resolution procedure can be formulated as a sequence of direction estimations and hypothesis tests. The estimation of the directions by the stochastic approximation is a rather simple procedure and compatible with the common array signal processing, because only independent steerable sum- and difference-beams are needed. The procedure is flexible for modifications. A multihypothesis test of sequential form (with respect to M) for the number of targets can be constructed, which has an approximate level of error for overestimating the number of targets. Computations and simulations showed that to resolve 2 targets separated by 0.5 beamwidth a reasonable signal-to-noise ratio of ca. 20dB is sufficient.

REFERENCES

1. Root, W.L., 1962, IRE Trans. Military Electr., April, 197-204.

2. Ksienski, A.A. and McGhee, R.B., 1968, IEEE Trans. AES-4, No.3, 443-455.

3. Birgenheier, R.A., 1972, Ph.D. dissertation University of California, Los Angeles.

4. White, W.D., 1974, IEEE Trans. AES-10, No.6, 835-852.

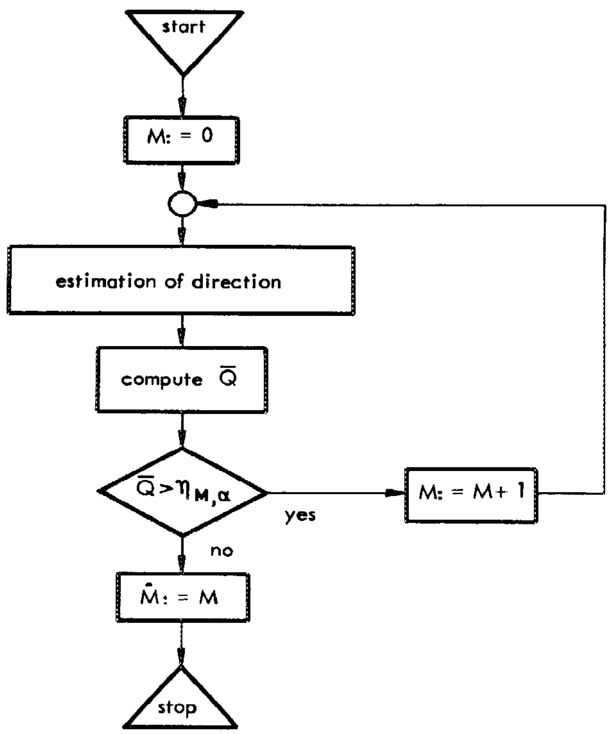

Figure 1. Resolution Algorithm

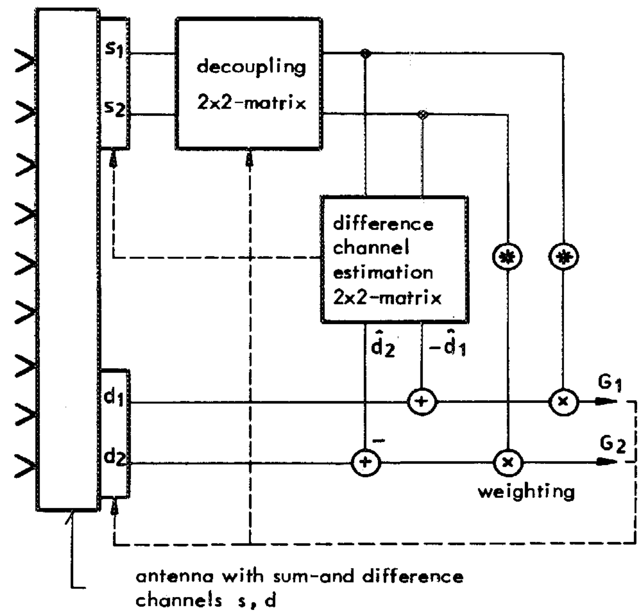

Figure 2. Computation of the Gradient

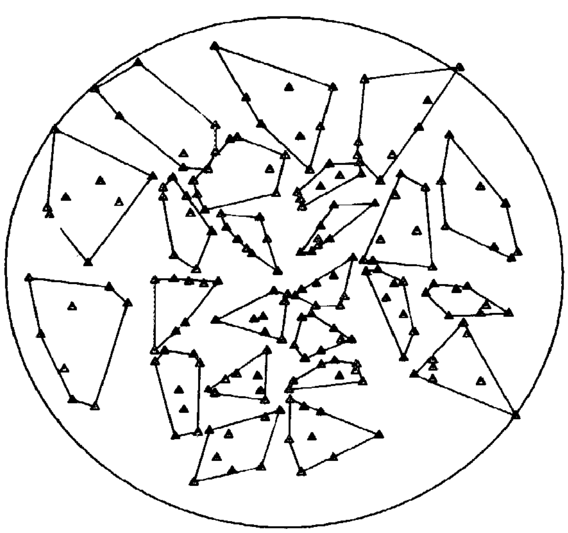

Diameter 32 λ

192 antenna elements arranged in 24 subgroups

Figure 3. Antenna Array

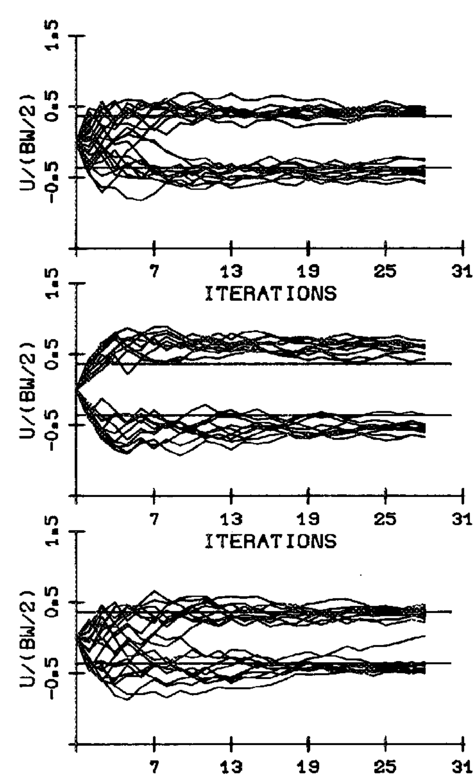

Figure 4. Computer Simulations

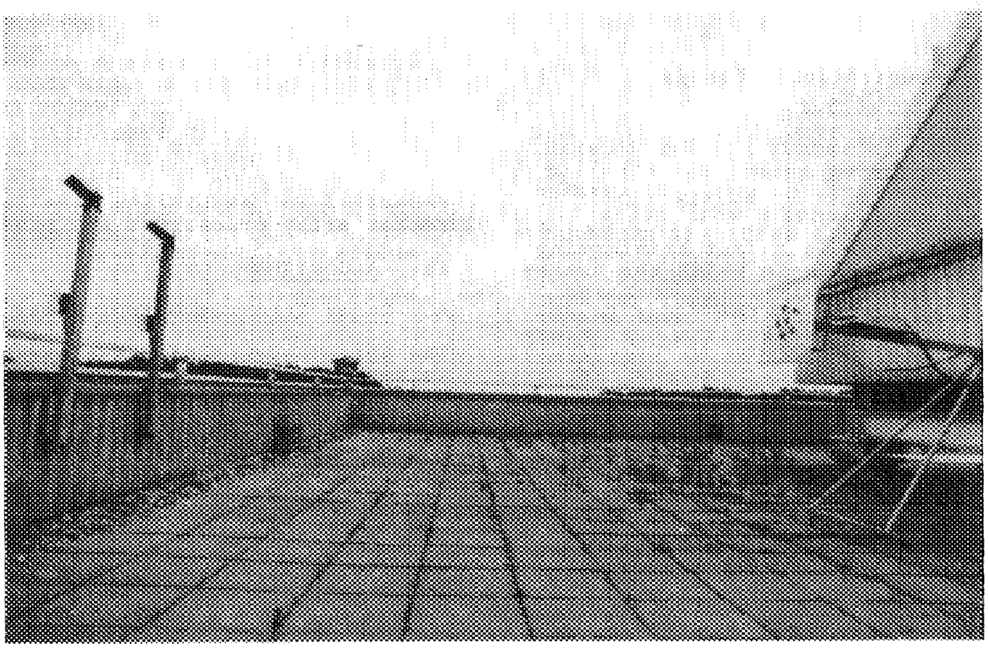

Figure 5. Arrangement of Measurement Equipment

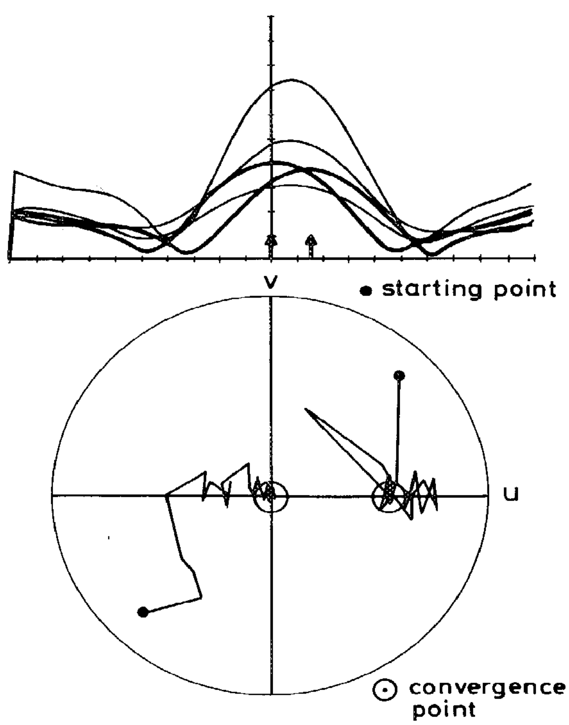

Figure 6. Estimation with measured Data

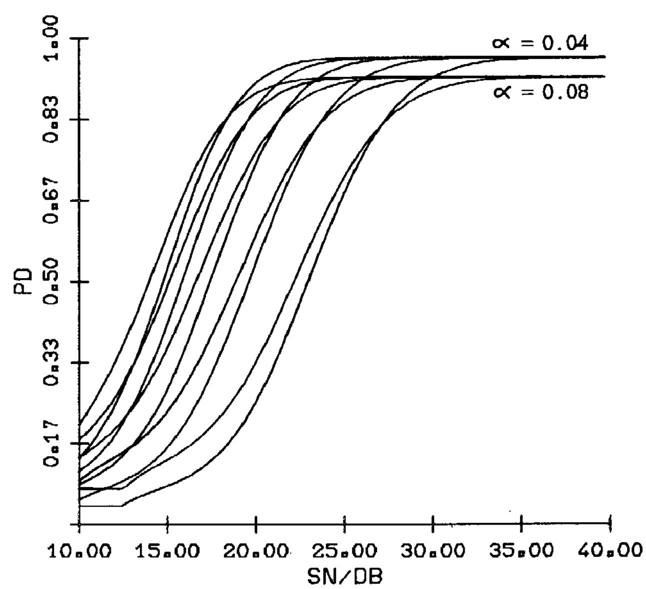

2 targets given at 0.5 BW separation

Figure 7. Computed Probability of Detection for 2 Targets